

Wide Field of View Telescope Array Space Object Detection With Artificial Intelligence And Image Restoration

He Zhao^{(1), (2)}, Rong-yu Sun⁽²⁾, Sheng-xian Yu⁽²⁾

⁽¹⁾ Purple Mountain Observatory, Chinese Academy of Sciences, Nanjing 210023, China, Email: hezhaopmo@pmo.ac.cn

⁽²⁾ School of Astronomy and Space Science, University of Science and Technology of China, Hefei, Anhui 230026, China

ABSTRACT

To meet the demand for object detection in a wide field of view for telescopes with many astronomical sources, we develop an Artificial Intelligence model to automatically find the streak object formed by the sidereal tracking observation mode. With manually labelled data set and improved neural network, preliminary result shows this case is feasible and has great potential. Besides, to deal with low signal-to-noise ratio (SNR) question, image restoration method with principal component/components analysis(PCA) point spread function(PSF) extraction. Results shows this method could increase the SNR and detect more object in test data.

1 Introduction

The earth orbit environment is getting complicated with the increasingly numerous artificial space vehicles for telecommunication, navigation weather report and science research, as shown in Fig. 1, posing pesky problems to model construction, aerospace operation and astronomical observation. Besides, the risk of collision between spacecrafts will increase, leading to the scattering of thousands of debris in near-Earth space. To avoid catastrophic consequence, it is significant to grasp the situation and changes in the space environment, which is also called Space Situation Awareness (SSA). Ground base optical observation is a key method wo achieve SSA, with the advantages of high efficiency and wide field of view, large-scale optical telescope is set around the world. And joint networking observation can better measure and track the space domain, such as European Union Space Surveillance and Tracking(EU SST), pace Surveillance Network (SSN) and International Scientific Optical Network(ISON). With the development of optomechanical technology, next generation facility will bring mass data in astronomical research. Brings opportunities and challenges to modern statistical methods represented by artificial intelligence.

Based on the data of wide filed of telescope array for multi-application in sidereal track mode, we build a neural network to detect the streak in the observation data ,besides to solve the low SNR question, image restoration method is tested on another data and start to perform potential.

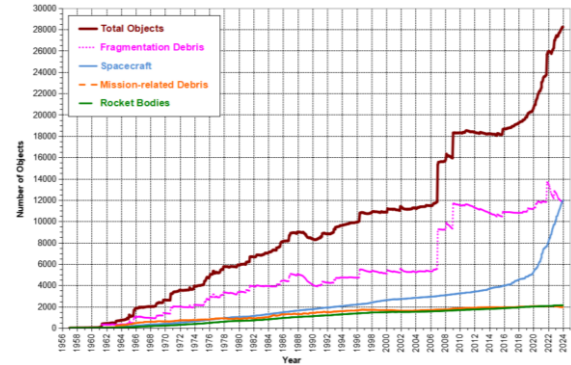


Figure 1. The number of catalogued space object increases with year

2 Hardware and Data

We are using a test facility of the telescope array, complete array will be available this year, the detail information of the telescope we used is shown in Tab.1, with the multi-application scientific objectives, this telescope is operating in sidereal tracking mode, survey the sky area. The survey azimuth is arranged from 107° to 251°, and the elevation is arranged from 12° to 45°.

Table 1.The information of the data

Parameter	Value
Diameter	700mm
Field of view	3.6°*3.6°
Sensor format	8120*8120
Pixel scale	1.6arcsec
Dynamic range	0-65535

Our observation covered ten nights, yielding a number of 30,476 fits file. In the future with complete telescope array the field of view and detection limit will be extended. Fig.2 shows the image capture by telescope. Differ from background star or galaxy point or spin-like, the space object will formed long or short streak morphology that space object in the Fig.2.

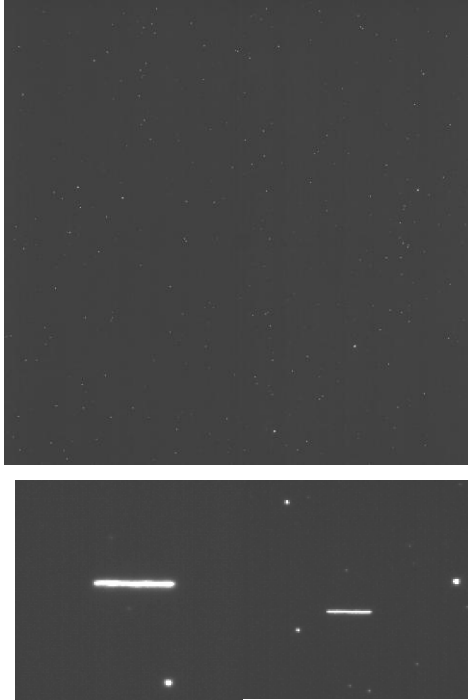


Figure 2. The image of the telescope and the morphology of the space object in this observation mode

3 Object detection method

3.1 Mixed of Experts(Moe)

Moe is a method for enhancing detection performance and efficiency by dynamically combining multiple sub-models (experts)[1]. Every experts represents a detecting unit, processing different tasks (such as classification, regression, multi-scale detection) or different target categories, enhancing the robustness of the model, the task will be allotted to one or more sub-models to give the sub-result, by combing the sub-result with weights the final result will be given. As shown in Fig.3. Besides with our multi-application data, those model can be migrated for other purpose like asteroids detection, transient source discovery and so on.

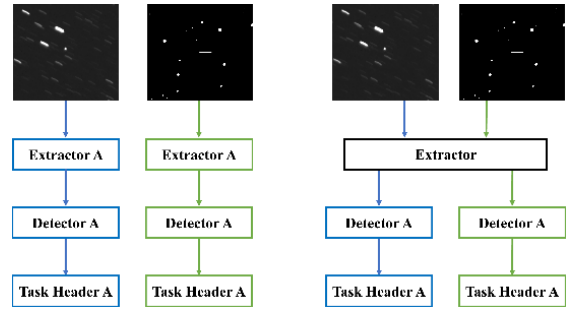


Figure3. Difference between the single model and unified model in space object detection. Left: single model Right: unified model(Mixed of Experts)

3.2 You Only Look Once(YOLO)

YOLO is a groundbreaking real-time object detection system that processes images in a single forward pass through a neural network. Introduced by Joseph Redmon et al. in 2016, YOLO revolutionized object detection by unifying localization (identifying object locations) and classification (recognizing object classes) into a single, end-to-end trainable model[2]. It is wide applied in various fields of life and science. For example, face recognition, autonomous driving, disaster alerts, detection of transient sources. And this model is still being updated and developed to this day. We have tested the performance of YOLO v5 on close-loop survey data with gaze mode for space object in point morphology[3].

3.3 Hungarian Algorithm

The Hungarian algorithm is a classical method for solving the optimal matching of weighted bipartite graphs. For a given $n \times m$ matrix, n represents assigned tasks and m represents recipients. $C_{n,m}$ represent the cost of n task to m recipients. This algorithm can solve the problem with maximum match, giving a minimum cost for all task, which will help in the point associate situation.

3.4 Application

To use this method, as typical neural network process, proprietary training set, training epoch, and test result will be introduced, we build a small feasible data set from the observation data, then we use this as training set in our Moe model, the well-trained model will be tested on the complete data of two nights, with the simple linear prediction and Hungarian Algorithm to solve the track problem, which will be described detailedly in the following paragraph.

3.4.1 Training set

Training set is of vital importance in the process of model validation because it is the feature of training set that be subtracted and learned by neural network and transfer to the new data and find what it has learned. So a good training set will benefit the application. However, in the object detection area, the construction of training set requires a large amount of manpower. For the reason that we are testing our method on the testing facility, it is appropriate to label a small amount of data. From all the data we picked 1200 image with steak object. Carefully labelled and a useful data set is constructed.

3.4.2 Training process

In the training process, our training set will be set into the neural network and the feature of our interested objected will be extracted and learned by the model and transfer to new data. The training process end when the loss function not decrease with epoch.

3.4.3 Object detection and track

20241010 and 20241011 is selected for test because these data over the past two days has been continuous images with five-second exposure. Moe with yolo will give the result of every possible object coordinate in the picture. For every sky area, as the short exposure time and observation interval, motion can be simply approximated as linear. At the first result, every coordinate will be set as a track, at next result, we will calculate a $n*m$ matrix represents the distance between each object in the two result, at this stage Hungarian Algorithm will give a result that one-to-one matching, then a threshold will be used to remove the match with large distance. Those points that exceeded the threshold will be set to a new track. If a track has two more points, the distance between the last two point will be calculate as the velocity and for a new result, the prediction that last location adding velocity times interval will be used to calculate the distance matrix, as shown in Fig 4.

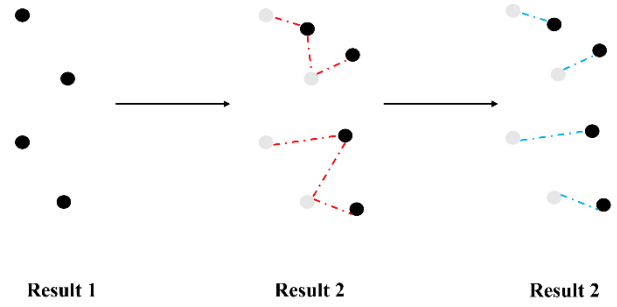
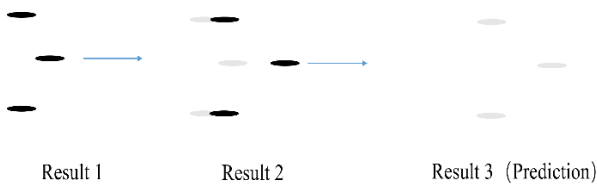


Figure 4. The tracking diagram

In a track if half of the result is missing, this track will be removed. After these steps, tracks from the same area will be selected.

4 Image Restoration

During the detection process we find that some object are overlooked for low SNR like Fig.4. To solve this problem , image restoration has been introduced and shown great performance in astrophysics research like galaxy morphology study and resolution of binary star systems. This method use image deconvolution to reduce the effect that PSF dispersed the energy of source. Depending on whether PSF is known, deconvolution is divided into unblind or blind. We have find a effective PSF subtract method from a large amount of data and shown this method can improve the astrometry accuracy[4].

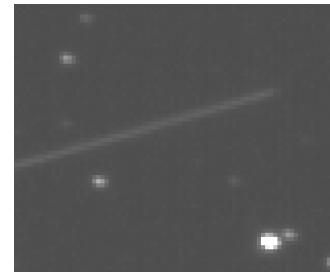


Figure 4. Object with low SNR

4.1 Deconvolution

Basic data formulation from (1)

$$I = H * O + N \quad (1)$$

Where I represents telescope image, O represents origin image, $*$ represents convolution, N represents noise. Try to reconstruct x from y .However , loss of high-frequency information and the presence of noise make direct recovery impossible ,called ill-posedness. Here three classical non-blind method is introduced.

4.1.1 Richardson-Lucy

Richardson-Lucy algorithm is a kind of expectation maximization method working in the spatial domain. The algorithm is based in Maximum Likelihood, and it gives a probability in (2)

$$p(I|O) = \prod_{x,y} \frac{[(P*O)(x,y)]^{I(x,y)} \exp\{-P*O(x,y)\}}{I(x,y)!} \quad (2)$$

To obtain the maximum value of $P(I|O)$. First take the logarithm of the above equation, and then take the derivative as (3).

$$\frac{\partial \ln p(I|O)(x,y)}{\partial O(x,y)} = 0 \quad (3)$$

As the PSF model is given and has been normalized, the estimation is solved iteratively:

$$\hat{O}_{k+1}(x,y) = \hat{O}_k(x,y) \left[P(x,y) * \frac{I(x,y)}{P*\hat{O}_k(x,y)} \right] \quad (4)$$

where $\hat{O}_{k+1}(x,y)$ is the posterior value of $O(x,y)$. However, for Richardson-Lucy algorithm, the iterative equation does not take into account noise, which means the restoration may converge to a result only containing the information of noise as the number of iterations increases. In addition, the ringing artifact appear as light strips around source edge will exist. To handle these challenges, additional regularization term is proposed to improve the estimation progress [5]. It is shown as (5)[6]

$$o_{k+1}(x) = \left\{ \left[\frac{i(x)}{(o_k * h)(x)} \right] * h(-x) - \lambda o_k(x) \ln(o_k(x)) \right\} \quad (5)$$

Here λ is set as 3×10^{-3} and the iteration number is 7

4.1.2 Maximum Entropy

For the maximum entropy method, the definition of entropy comes from information theory, which is shown as (6).

$$H = - \sum_x \sum_v O(x,y) \ln O(x,y) \quad (6)$$

To maximize H , the Lagrange Multiplier is adopted, and the estimation process is described as (7).

$$\begin{aligned} \hat{O}_k(x,y) &= c \exp(\lambda_k^L * P(x,y)) \\ \lambda_{k+1}^L &= \lambda_k^L + \Delta \lambda_k^L \\ \Delta \lambda_k^L &= \log I(x,y) - \log (P(x,y) * \hat{O}_k(x,y)) \end{aligned} \quad (7)$$

where λ^L is the Lagrange Multiplier

4.1.3 Wiener filtering

The last image restoration method used in our research is Wiener filtering. It works in Fourier space, the imaging equation can be transformed as (8):

$$\hat{I}(u,v) = \hat{H}(u,v) \times \hat{O}(u,v) + \hat{N}(u,v) \quad (8)$$

Here $\hat{H}(u,v)$, $\hat{I}(u,v)$, $\hat{O}(u,v)$ and $\hat{N}(u,v)$ are the transforms of the $H(x,y)$, $I(x,y)$, $O(x,y)$ and $N(x,y)$ respectively. The principle of wiener filtering is

minimizing the mean square error between the 'real' image $O(x,y)$ and degraded image $I(x,y)$. The solution is obtained by(9):

$$\hat{O}(u,v) = \frac{\hat{H}^*(u,v)\hat{I}(u,v)}{|\hat{H}(u,v)|^2 + \sigma_N^2(u,v)/\sigma_O^2(u,v)} \quad (9)$$

4.1.4 Neural Network

Besides these, Artificial Intelligence can be used in this process because this process has no strict mathematical expression, this end-to-end method may reproduce this process. And has been widely used in life like photo fuzzy repair. Since the deconvolution method does not provide precise expression, using a neural network as a black box is appropriate. We choose a U-net construct which is commonly used in image generation, shown in Fig.5. In our process, the data with known PSF convolution will be put as training set, and the origin data will be set as target set, in the iterative training process the deconvolution is learned by the neural network, when the training process is done, the origin data is sent into the neural network and may receive the deconvolution result.

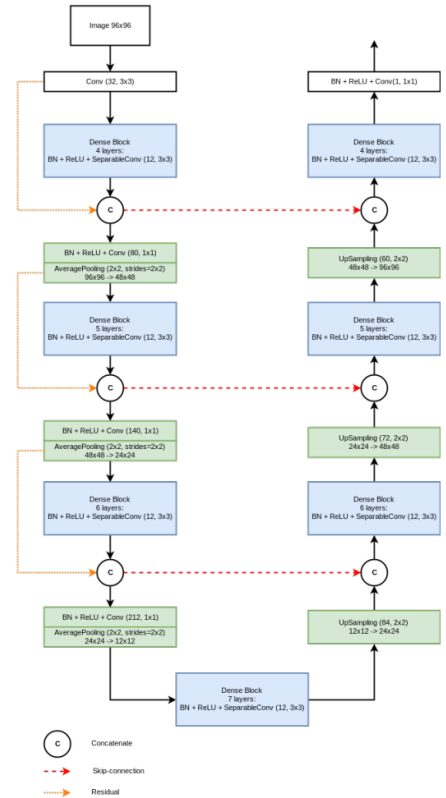


Figure 5. The structure of U-net

4.2 PSF models

As mentioned previously, the PSF model plays

important roles in image restoration. As the PSF describes the characteristics of the imaging system, besides the classic empirical models, deriving PSF from observational images is also an efficient and reliable way. Several techniques are proposed to extract the PSF from large numbers of raw data, and PCA is one of them[7]. It has been widely applied in a number of astronomical applications[8]. The aim of PCA is obtaining the optimal set of basis from large numbers of data with dimensionality reduction, as wide field of view provides large number of background star images, it is feasible to perform PCA.

As mentioned previously, the PSF model plays significant roles in image restoration. As the PSF describes the characteristics of the imaging system, besides the classic empirical models, deriving PSF from observational images is also an efficient and reliable way. Several techniques are proposed to extract the PSF from large numbers of raw data, and PCA is one of them[7]. It has been widely applied in a number of astronomical applications[9]. The aim of PCA is obtaining the optimal set of basis from large numbers of data with dimensionality reduction, as wide field of view provides large number of background star images, it is feasible to perform PCA

To evaluate the performance of different PSF models, in our research the Gaussian model, Moffat model and model obtained with PCA are used. The Gaussian model and Moffat model are generated by `Gaussian2DKernel` and `Moffat2DKernel` of `astropy`. For Gaussian model, the mean is set as 0 and the variance is set as 1, without any modified functions. For Moffat model, the core width γ is set as 3, and the power index α is set as 1:5. The construction of PSF model with PCA is the same with the application in our former research [9]. First a large number of sidereal-tracking images is obtained, and the sources are extracted as samples, each sample is a two-dimensional array taking the peak value pixel as center. After background subtraction and normalization, the the singular value decomposition (SVD) is performed. Assuming N PSF samples are obtained and each sample consists of M values, the matrix S is constructed with N rows and M columns, each row of S is a PSF sample presented in one dimension. For each column of S , the decomposition is performed as follows:

$$S^2 = UWV^T \quad (10)$$

where U is a $N \times M$ column-orthogonal matrix, W is a $M \times M$ diagonal matrix, and V is a $M \times M$ orthogonal matrix. Each column of V^T is a decomposed PSF component with the same size as PSF samples, and the relative weights of these components are presented as the diagonal elements of W . The indexes show the order of the PSF components. The first component has the maximum weight and the ones with high indexes are mainly noises. The relative

weights of the effective components drop dramatically in high order components, hence after arranging the PSF components according to their weights, the effective ones are selected and generated to the final PSF model adopted in restoration

The three PSF models used in image restoration are shown in Fig.6. It should be noted that both the Gaussian model and Moffat model are symmetrical, while the PCA model is asymmetric.

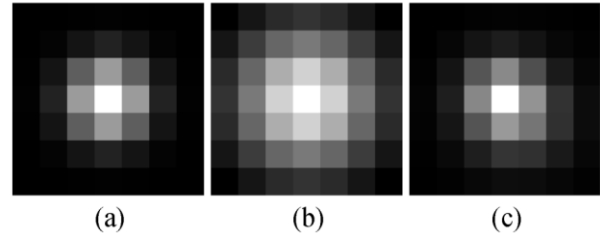


Figure 6. The three PSF models used in image restoration. (a): Gaussian. (b): Moffat. (c): PCA

5 Results and Discussion

5.1 Object detection

The detected and correlated result is shown in Tab.2.

Table 2.The result of the method

Date	20241010	20241011
Fits number	4678	4997
Result number	4433	2855
Detection number	31356	6877
Track number	2811	595
Tracker detection number	27670	5209

As the results shows our method can detect the streak targets in new data and track method will successfully correlate the object between frame in the same sky area and filter out abnormal detection points. The association with the database is not yet complete for various reasons. We sampled the track pas and confirm that it is indeed a space object based on its shape and motion characteristics.

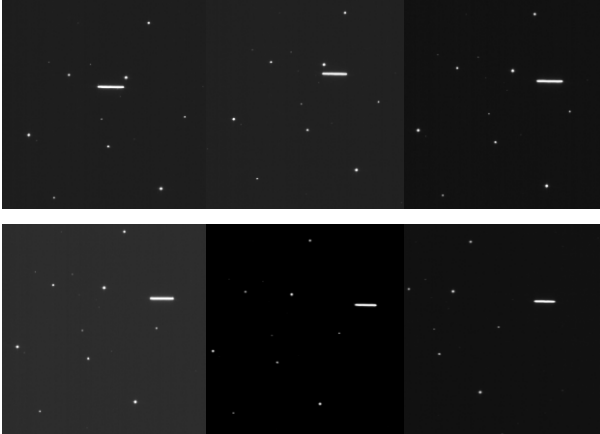


Figure 7. The tracking result

Fig.7 shows the object motion between continuous frame. With the reason of observation, the result of second day is poor. We will carefully analysis in the future work.

5.2 Image Restoration

Combine different methods with PSF, the object detection capability is improved ,the number of detected object is improved, as shown in Fig.8.

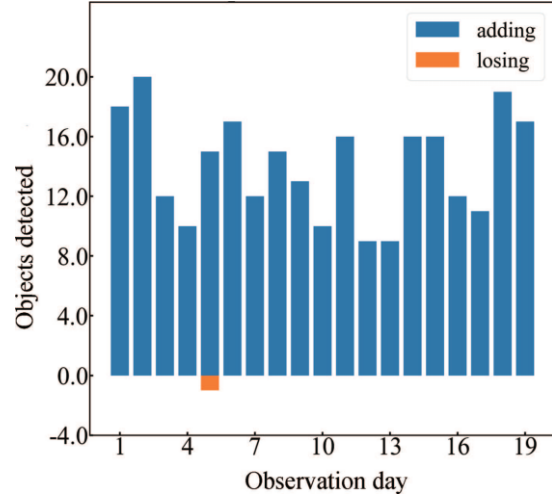


Figure 8. The count of newly detected and lost objects after binning of the results from multiple restoration methods and PSF models

For the neural network, some star morphology is changed with square, as shown in Fig.9. It may be cause by the generation method ignoring the noise effect. Future work will consider more complex patterns and more advanced tools.

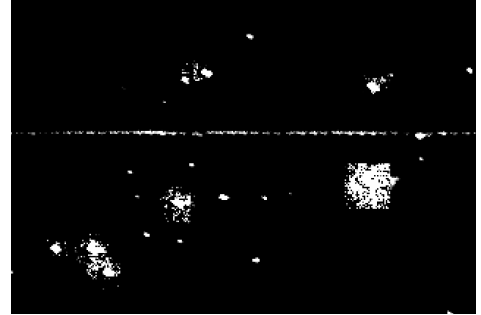


Figure 9. The square phenomenon in the restoration process

However, for our object with smaller contour features, the morphology is impacted slightly, due to time constraints, subsequent track associations were not performed, the SNR is calculated and the result is shown in Fig.10. It can be seen that the SNR is improved by this method.

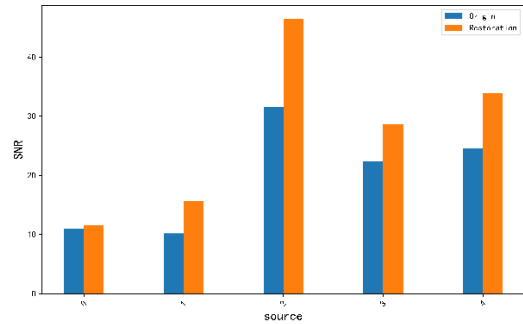


Figure 10. The SNR of space object

6 Conclusion

With the newly built telescope array, we test the AI-based streak-like space object detector and tracker, we believe the Moe and Yolo will play a unique role in the future application. On the other side, for the low SNR target, image restoration method is applied to improve the detect limit, classical method performed the feasibility and result shows the deep learning method can improve the SNR for target, future research will show systematic result for application,

7 REFERENCES

1. Li, Y., Li, X., Li, Y., Zhang, Y., Dai, Y., Hou, Q., ... & Yang, J. (2024). Sm3det: A unified model for multi-modal remote sensing object detection. *arXiv preprint arXiv:2412.20665*.
2. Redmon, J., Divvala, S., Girshick, R., & Farhadi, A. (2016). You only look once: Unified, real-time object detection. In *Proceedings of the IEEE conference on computer vision and pattern recognition* (pp. 779-788).
3. Zhao, H., Sun, R. Y., & Yu, S. X. (2024). Deep Neural Network Closed-loop with Raw Data for Optical Resident Space Object Detection. *Research in Astronomy and Astrophysics*, 24(11), 115009
4. Sun, R., Yu, S., Jia, P., & Zhao, C. (2020). Improving position accuracy for telescopes with small aperture and wide field of view utilizing point spread function modelling. *Monthly Notices of the Royal Astronomical Society*, 497(3), 4000-4008.
5. Dey, N., Blanc-Feraud, L., Zimmer, C., Roux, P., Kam, Z., Olivo-Marin, J. C., & Zerubia, J. (2006). Richardson–Lucy algorithm with total variation regularization for 3D confocal microscope deconvolution. *Microscopy research and technique*, 69(4), 260-266.
6. De Monvel, J. B., Le Calvez, S., & Ulfendahl, M. (2001). Image restoration for confocal microscopy: improving the limits of deconvolution, with application to the visualization of the mammalian hearing organ. *Biophysical Journal*, 80(5), 2455-2470.
7. Jee, M. J., Blakeslee, J. P., Sirianni, M., Martel, A. R., White, R. L., & Ford, H. C. (2007). Principal component analysis of the time-and position-dependent point-spread function of the advanced camera for surveys. *Publications of the Astronomical Society of the Pacific*, 119(862), 1403.
8. Jee, M. J., & Tyson, J. A. (2011). Toward precision LSST weak-lensing measurement. I. Impacts of atmospheric turbulence and optical aberration. *Publications of the Astronomical Society of the Pacific*, 123(903), 596.
9. Sun, R.-y., Yu, P.-p., & Zhang, W. (2022). Precise position measurement for resident space object with point spread function modeling. *Adv. Space Res.*, 70, 2315–2322.